HAYATI
Journal of Biosciences

Vol. 28 No. 4, October 2021 271-285
DOI:10.4308/hjb.28.4.271-285
ISSN: 1978-3019
EISSN: 2086-4094

Modeling Mackerel Tuna (*Euthynnus affinis*) Habitat in Southern Coast of Java: Influence of Seasonal Upwelling and Negative IOD

Alan F Koropitan[1*], Ibrahim Kholilullah[1], Roza Yusfiandayani[2]

[1]*Department of Marine Science and Technology, Faculty of Fisheries and Marine Sciences, IPB University, Bogor, Indonesia*
[2]*Department of Fisheries Resources Utilization, Faculty of Fisheries and Marine Sciences, IPB University, Bogor, Indonesia*

ARTICLE INFO

Article history:
Received September 15, 2020
Received in revised form July 5, 2021
Accepted August 30, 2021

KEYWORDS:
extreme negative IOD 2016,
GAM,
upwelling,
mackerel tuna,
southern coast of Java

ABSTRACT

We used fishery catch data from Cilacap Fishing Port and Copernicus data set in July 2016-December 2017 to investigate the impacts of Indian Ocean Dipole (IOD) on upwelling and mackerel tuna distribution in the southern coast of Java. This study implemented a Generalized Additive Model (GAM) for habitat prediction of mackerel tuna in the waters. The present study showed that the extreme negative IOD in 2016 caused a weaker southeasterly wind and even a reversal to the northwesterly wind, as seen off Sumatra in September 2016. The situation produced vertically mixed layer thickening and no upwelling during the southeast monsoon event 2016, consequently resulted in warmer temperature and fewer Chlorophyll-a (Chl-a) compared to the southeast monsoon event 2017. The mackerel tuna production significantly dropped in 2016 and rose in 2017, particularly during the upwelling event. The high Habitat Suitability Index (HSI) was found in southern Central Java in July 2017, expanded bigger in August 2017, and decreased in September 2017. During July and August 2016, the high HSI covered only a less area in the region and disappeared in September 2017. The high HSI indicates that the oceanographic factor is consistent with the catch probability of mackerel tuna.

1. Introduction

The success of fishing is affected by the ability of the fishermen to choose their fishing ground. Especially for the traditional fisherman, past experiences often become a reference for fishing in the ocean. Meanwhile, fish production and distribution in the sea are under control by the oceanographic processes and fisheries biology. Oceanography deals with ocean current, material transport, fish forage distribution, and climate variability, while the early life of fish, recruitment, and mortality (natural and fishing) are the key elements for fisheries biology. In the simple food chain, phytoplankton is located at the lowest trophic level and requires nutrients and sunlight for their growth. Chl-a concentration as an indicator of phytoplankton biomass could use for assessing the availability of the forage. The complex interaction between oceanography and fisheries biology needs to resolve for sustainable fisheries management. However, it is hard to understand by the fishermen, so they need a tool in bridging oceanography and fisheries biology.

The upwelling phenomenon plays a significant role in nutrients supply widely along coastal seas. It has already known that the seasonal upwelling in the Indonesian seas occurs during the peak of the southeast monsoon in June-August, as described in detail by Wyrtki (1961). Since then, the upwelling dynamics in the Indonesian seas have been investigating by several studies, which is at the southern coast of Java-Lesser Sunda Islands (Susanto *et al.* 2001; Potemra *et al.* 2003; Chen *et al.* 2016; Varela *et al.* 2016; Taufikurahman and Hidayat 2017; Wirasatriya *et al.* 2020; Xu *et al.* 2021), and Banda Sea (Gordon and Susanto 2001; Rachman *et al.* 2020).

Related to upwelling, in brief, water mass in the surface moves at a 90° angle from the direction of the wind, which is as a net transport to the right (left) of the wind direction in the northern (southern) hemisphere. The upwelling along the southern coast of Java-Lesser Sunda Islands is forced by a southeasterly wind. Therefore, the surface water masses in the

* Corresponding Author
E-mail Address: alan@apps.ipb.ac.id

southern hemisphere move toward the offshore called Ekman transport. As compensation, it triggers the rise of water masses from the deep layer to the surface layer (Ekman pumping), and consequently, it brings cold and nutrient-rich water and increases phytoplankton biomass (and Chl-a concentration) in the surface layer. It implies that the southeast monsoon coincides with high fish production in the region (Lahlali *et al.* 2018). In this case, the southern coast of Java is known as productive fishing grounds for tuna due to the coastal upwelling (Syamsuddin *et al.* 2016; Lahlali *et al.* 2018).

Previous studies have reported that upwelling in the region is also modulated by interannual variabilities, such as El Niño-Southern Oscillation (ENSO) and Indian Ocean Dipole (IOD) (Susanto *et al.* 2001; Wirasatriya *et al.* 2020; Xu *et al.* 2021). For a simple explanation, during El Niño, the relatively warm surface water in the eastern Indonesian seas moves to the central Pacific Ocean or positive (negative) anomaly of sea surface temperature (SST) in the central Pacific Ocean (the Indonesian seas). Reversely, during La Niña, the warm surface water moves into the Indonesian seas. It means El Niño (La Niña) has a longer dry season (rainy season) in the Indonesian seas. Similarly, in the Indian Ocean, positive IOD refers to El Niño, while negative IOD refers to La Niña in the Pacific Ocean. A positive IOD means that SST in the south of Java and west of Sumatra is cooler than usual (negative anomaly), while the tropical central-western Indian Ocean is warmer than usual (positive anomaly) and vice versa during a negative IOD.

In addition to the upwelling dynamic, other aspects that emphasized regarding ENSO and IOD modulation include rainfall (Nur'utami and Hidayat 2016), SST variability, as well as dynamics and predictability (Lim and Hendon 2017; Iskandar *et al.* 2018; Lu *et al.* 2018; Kämpf and Kavi 2019). Several studies on the impacts of ENSO and IOD on tuna include Lan *et al.* (2013), Lumban Gaol *et al.* (2015), Báez *et al.* (2020), Wu *et al.* (2020), Wiryawan *et al.* (2020). Most recently, Lumban Gaol *et al.* (2021) examined the effect of IOD and monsoon events on upwelling-downwelling and small pelagic fish in terms of salinity, temperature, Chl-a, and using monthly catch data in the southern coast of Java. However, only a little attention has examined the effect on mackerel tuna. The present study aims to investigate the impacts of negative IOD on seasonal coastal upwelling and mackerel tuna productions in the southern coast of Java, as well as to determine the mackerel tuna habitat by using GAM. The model can be a tool in assessing fish habitat, characterized by oceanographic parameters and productivity of fish catch.

2. Materials and Methods

The present study focuses on the fishing grounds in the area where the Indonesian fishing vessels operate on the southern coast of Java, particularly the landed base at Cilacap Fishing Port. The model region of this study covers the coordinates 5°-13°S and 90°-120°E. However, the model region of mackerel tuna habitat covers the southern coast of Java-Lesser Sunda Islands (Figure 1).

The data used are catch data and oceanographic data. Mackerel tuna daily catch data was obtained from Cilacap Fishing Port for the period of July 2016 to December 2017 and were digitized from fishing log-book of three fishing gears (longline, gillnet, and hook and line) from 1999 samples and compiled into a database. The data consisted of daily geo-referenced fishing positions (latitude and longitude), catch in kg, and effort from which catch per unit effort (CPUE). The CPUE was calculated according to Sparre and Venema (1999) is as follows:

$$CPUE = C/F \qquad (1)$$

Where:
C (catch) = is the total catch (kg)
F (Effort) = is the total fishing effort taken from the length of the fishing trip (days)

The CPUE is determined in kg per trip, while the CPUE data are divided into four classes based on the data quartile (Chen *et al.* 2005). We used the total CPUE of the three fishing gears, where the GL fishing gear contributes 86% of the total CPUE.

This study has been conducted using E.U. Copernicus Marine Service Information. The Oceanographic data products or derivative works of the Copernicus were downloaded for particular parameters (accessed on 22 August 2021), such as SST, sea surface Chl-a (SSC), eddy kinetic energy (EKE), mixed layer depth (MLD), and sea surface salinity (SSS). All parameters are in

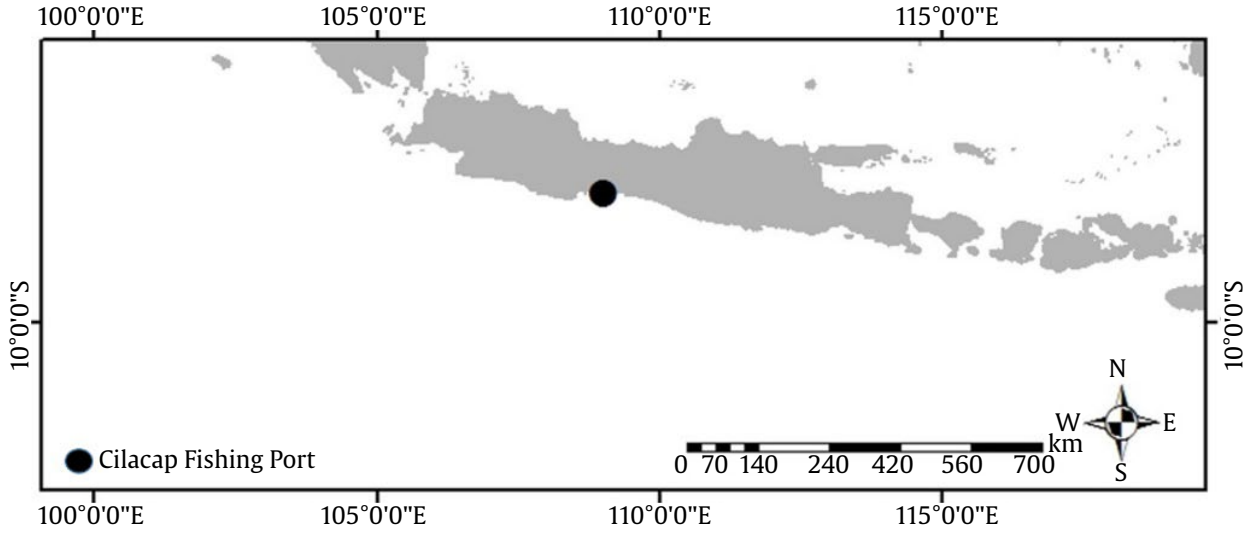

Figure 1. Study area in the southern coast of Java-Lesser Sunda Islands

daily-mean temporal resolution and monthly averaged calculation was performed for data analysis. SST, MLD, and SSS were taken from GLOBAL_REANALYSIS_PHY_001_030 with a spatial resolution of 0.083° by 0.083°. SSC, geostrophic current and surface current were adopted from OCEANCOLOUR_GLO_CHL_L4_NRT_OBSERVATIONS_009_033 (4 by 4 km), SEALEVEL_GLO_PHY_L4_REP_OBSERVATIONS_008_047 (0.25° by 0.25°), and GLOBAL_ANALYSIS_FORECAST_PHY_001_024 (0.083° by 0.083°), respectively. EKE calculation is according to the following equations (Wang *et al.* 2017):

$$EKE = 0.5 (\mu'^2 + v'^2) \quad (2)$$

$$\mu' = u-U, v' = v-V \quad (3)$$

All parameters were re-sampled to the higher resolution, refer to Chl-a data set (4 by 4 km) and subset to the study area. The oceanographic and fishing data were processed and visualized using PyFerret, Ocean Data View (Schlitzer 2021), and ArcGIS 10.8.1. PyFerret is a product of NOAA's Pacific Marine Environmental Laboratory (Information is available at http://ferret.pmel.noaa.gov/Ferret/).

GAMs were constructed in R 3.5.0 (R Core Team 2018) software, using the gam function of the mgcv package (Wood 2006), with CPUE as the response variable and SST, SSC, SSS, EKE and MLD as predictor variables. The model is shown in equation (4):

$$g(u_i) = \alpha_0 + s_1(x_{1i}) + s_2(x_{2i}) + s_3(x_{3i}) + ...s_n(x_{ni}) \quad (4)$$

Where:
g = is the link function
ui = is the expected value of the dependent variable (CPUE)
$\alpha 0$ = is the model constant, and sn is a smoothing function for each of the model covariates x_n

A logarithmic transformation on CPUEs to normalize the asymmetrical distribution is adopted according to Zainuddin *et al.* (2008). After constructing GAM, the predict gam function in mgcv package was performed to predict mackerel tuna CPUEs, given a set of covariates similar to those used to build the model. This approach was employed as informed by Mugo *et al.* (2010), Howell and Kobayashi (2006), and Zagaglia *et al.* (2004).

3. Results

3.1. Oceanographic Features

The wind is the main generating force for upwelling, also known as Ekman transport. Wind patterns in July, August and September (JAS) 2016 and 2017 are presented in Figure 2. The southeasterly wind in the study area has a spatially different distribution pattern, where it is generally slower in the eastern part than in the western part. The distribution pattern was seen both in 2016 and 2017. However, a weakening wind magnitude occurred in 2016 compared to 2017, and even a reversal of the wind direction to northwesterly wind occurred around the western coast of Sumatra in September 2016. The southeasterly wind magnitude was dominated by more than 10.0 m/s in 2017, while it was only around 6-8 m/s in 2016. The result of windrose analysis at the selected position (Figure 3) shows that the wind magnitude in 2017 was dominated by 5.70-8.80 m/s at

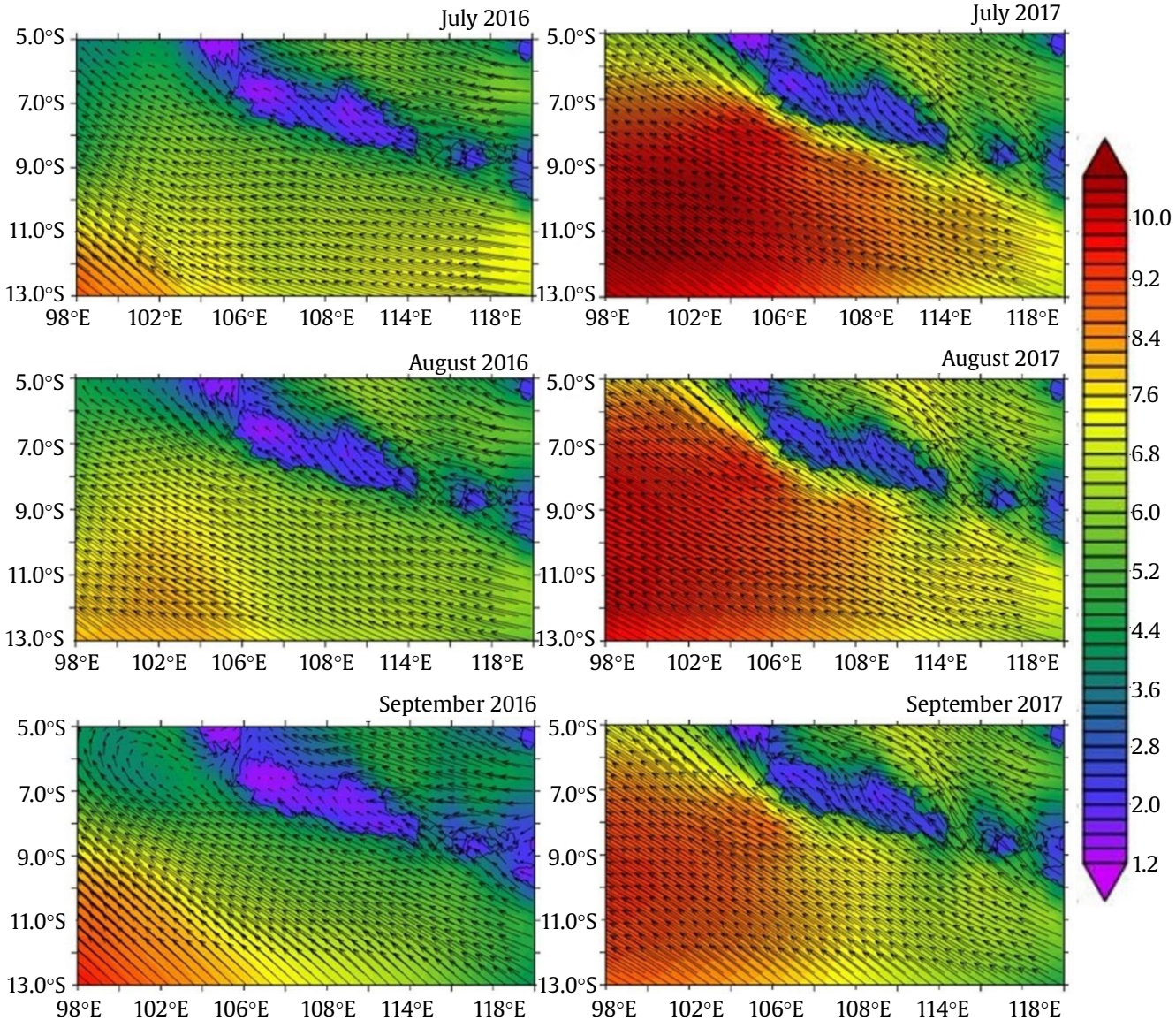

Figure 2. Monthly averaged of wind pattern (m/s) during JAS 2016 and 2017

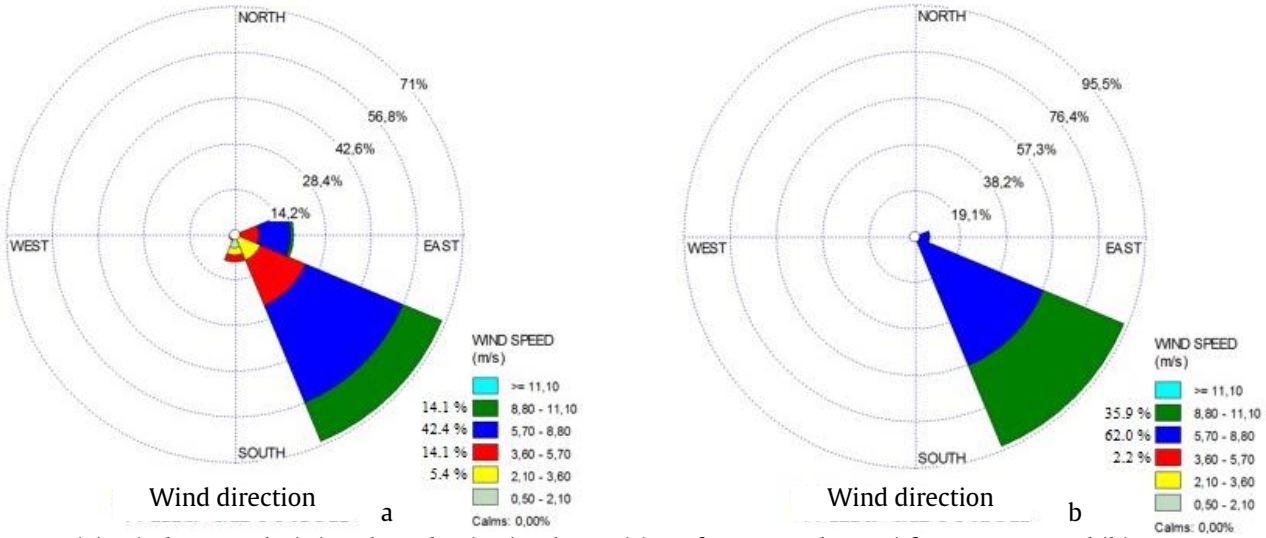

Figure 3. (a) Windrose analysis in selected point (at the position of 108° E and 8.6° S) for JAS 2016, and (b) 2017

62%, followed by wind magnitude of 8.80-11.10 m/s at 35.9% and only around 2.2% wind magnitude 3.6-5.7 m/s. In 2016 (extreme negative IOD), the wind magnitude was dominated by 5.7-8.8 m/s at 42.4%, followed by wind magnitude at 3.6-5.7 m/s at 26.1%, and 8.8-11 m/s at 14%. In addition to 2016, it also showed weaker wind magnitude of 2.1-3.6 m/s at 12% and 0.5-2.10% at 5.4%.

The impact of the southeasterly wind affects the MLD in the study area. In general, the stronger the wind, the deeper the MLD due to turbulence that mixes the water masses from the surface layer to the thermocline depth. On the other hand, the stronger the southeasterly wind, the greater the coastal upwelling magnitude, so that the thermocline layer rises. A cross-section profile of temperature in the study area (Figure 4) represents the interaction of these two things. The cross-section profile shows a mixed layer depth at 100 m in the west, where the slope rises gently to the east until 115°E during JAS 2016. In addition, the shallow mixed layer depth at around 40-60 m occurs in the west during JAS 2017, where the slope rises steeply to the east until 115°E. So, the impact of extreme negative IOD in 2016 has produced the westerly wind anomalies, that reduces the wind magnitude in the western coast of Sumatra

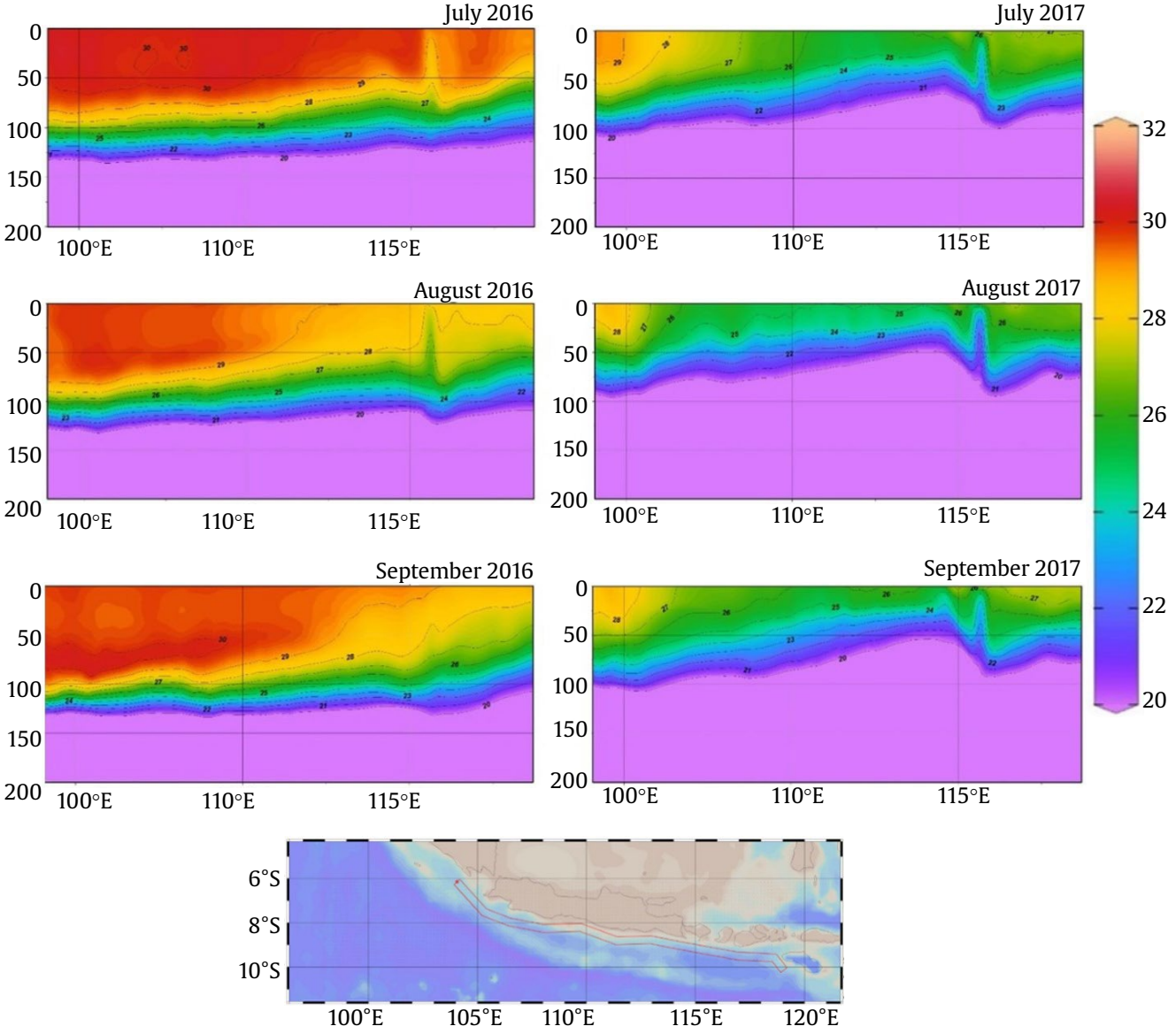

Figure 4. Cross-section profile of monthly-mean temperature along the southern coast of Java-Lesser Sunda Islands during JAS 2016 and 2017. The Lombok strait is located around 115.2°-115.8°E.

(Figure 2). At last, it deepens the thermocline in the west part of the study area (Figure 4).

Figure 4 also highlights a strong mixing at the entrance to narrow Lombok Strait, which has a sill depth of about 250 m. Our results found less mixing in September 2016 compared to September 2017. The less mixing might be affected by the weakening of the southeasterly wind in September 2016, subsequently reducing the upwelling magnitude and increasing the mixed layer depth in the entrance of Lombok Strait. The strong mixing is seen to resume at the entrance of Lombok Strait in JAS 2017 due to the increasing upwelling magnitude that pumps up the thermocline layer.

The decrease in wind magnitude as generating force of upwelling and mixed layer thickening, result in no upwelling during extreme negative IOD. Furthermore, the presence or absence of upwelling could be confirmed through the distribution of SST, as shown in Figure 5. During JAS 2016, it has detected a monthly SST of >29°C in parts of the western coast of Sumatra and the southern coast of Java, including Sunda Strait. This warmed SST is the effect of the negative IOD that extends to the Java Sea and the Java upwelling system area.

There was no warmed monthly SST during JAS 2017, as shown by the presence of cold monthly SST at <24°C in parts of the southern coast of Java as well as Bali and Lombok. The cold waters indicate an upwelling in the region. In general, Figure 5 presents a relatively different SST between the eastern and western parts of the study area during JAS 2016 and 2017. The SST at the east is lower than those at the west.

As mentioned in the introduction, the observation of Chl-a bloom can be an indicator of upwelling events. Figure 6 shows the monthly mean of remotely-sensed Chl-a in JAS 2016 and 2017. During the JAS 2016, Chl-a blooms were almost not seen in the study area, except for a small part in the southern Bali Strait in August 2016 which detected a monthly mean of Chl-a concentrations >1 mg/m^3. The decrease in the intensity of Chl-a bloom was influenced by the extreme negative IOD as previously mentioned.

In contrast to the JAS 2016, the concentration of Chl-a bloom (>1 mg/m^3) began to be seen sporadically in southern Java to Bali-Lombok Islands in July 2017. In August 2017, the concentration of Chl-a bloom began to consolidate and spread to the west coast of southern Sumatera and the entire Lesser Sunda Islands. However, in September 2017, the distribution began to decrease, although the consolidation is still visible along the south coasts of Java and the Lesser Sunda Islands.

3.2. Modeling Habitat

Figure 7 presents the calculated CPUE at the Cilacap Fishing Port. The peak CPUE was seen in July until September 2017 with range of 40,000-60,000 kg/trip, while the lowest value occurred in January 2017 at 138 kg/trip. The increase in CPUE started in May 2017 and decreased significantly from September to December 2017. However, in July–September 2016, it did not show performance as in 2017, there was no significant increase in CPUE. As discussed in the introduction, the effect of upwelling might control the CPUE variability, which occurs in the southeast monsoon period. The peak CPUE in July-September 2017 has a 1-month lag referred to the peak of southeast monsoon in June-August. Especially for 2016, the impact of negative IOD might produce low CPUE in the region and consistent with the negative IOD event that peaked in July-September.

The distribution of CPUE in the study area during JAS 2016 and 2017 is presented in Figure 8. The comparison of CPUE distributions between 2016 and 2017 is very contrasting, where the CPUE concentrates only in one area (central part of the southern coast of Java) with a high CPUE in 2017 (>102.85 kg/trip). On the other hand, the CPUE rarely scatters with a much lower CPUE (0.01-28.23 kg/trip) during the extreme negative IOD of JAS 2016.

The results of HSI model for mackerel tuna in JAS 2016 and 2017 are presented in Figure 9. The Java

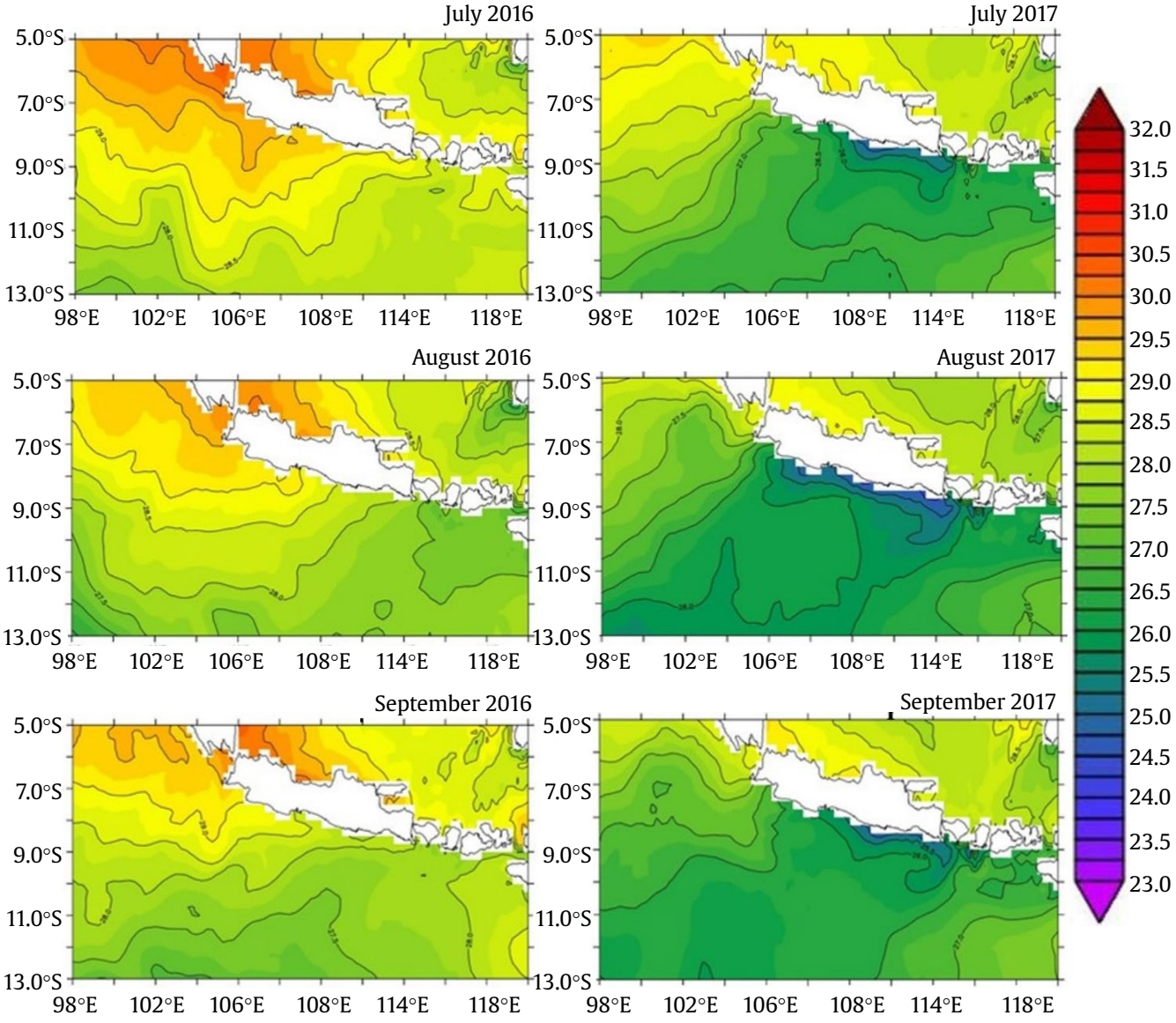

Figure 5. Monthly averaged of SST distribution (°C) during JAS 2016 and 2017

Sea waters are not considered in the discussion of this study. This case avoids overestimating fishing predictions caused by overestimating remotely-sensed Chl-a concentrations that often occur in turbid waters such as the Java Sea due to many riverine inputs. The HSI range between 0 and 1, where the higher the HSI value, the more suitable the environmental conditions (oceanography) to become their habitat. Therefore, the HSI provides a reference location as a fishing ground.

At the peak of the southeast monsoon event in 2017, the calculated HSI shows a distribution of high values of 0.5-0.6 (yellow shaded) in southern Central Java and southern Bali-Lombok Straits in July 2017 (Figure 9 and 10). The high HSI distribution in the regions expands bigger during August 2017 and only remains in southern Bali-Lombok Strait in September 2017 (Figure 10). However, the HSI value of 0.4-0.5 (bright green shaded) still distributes in the south of Central

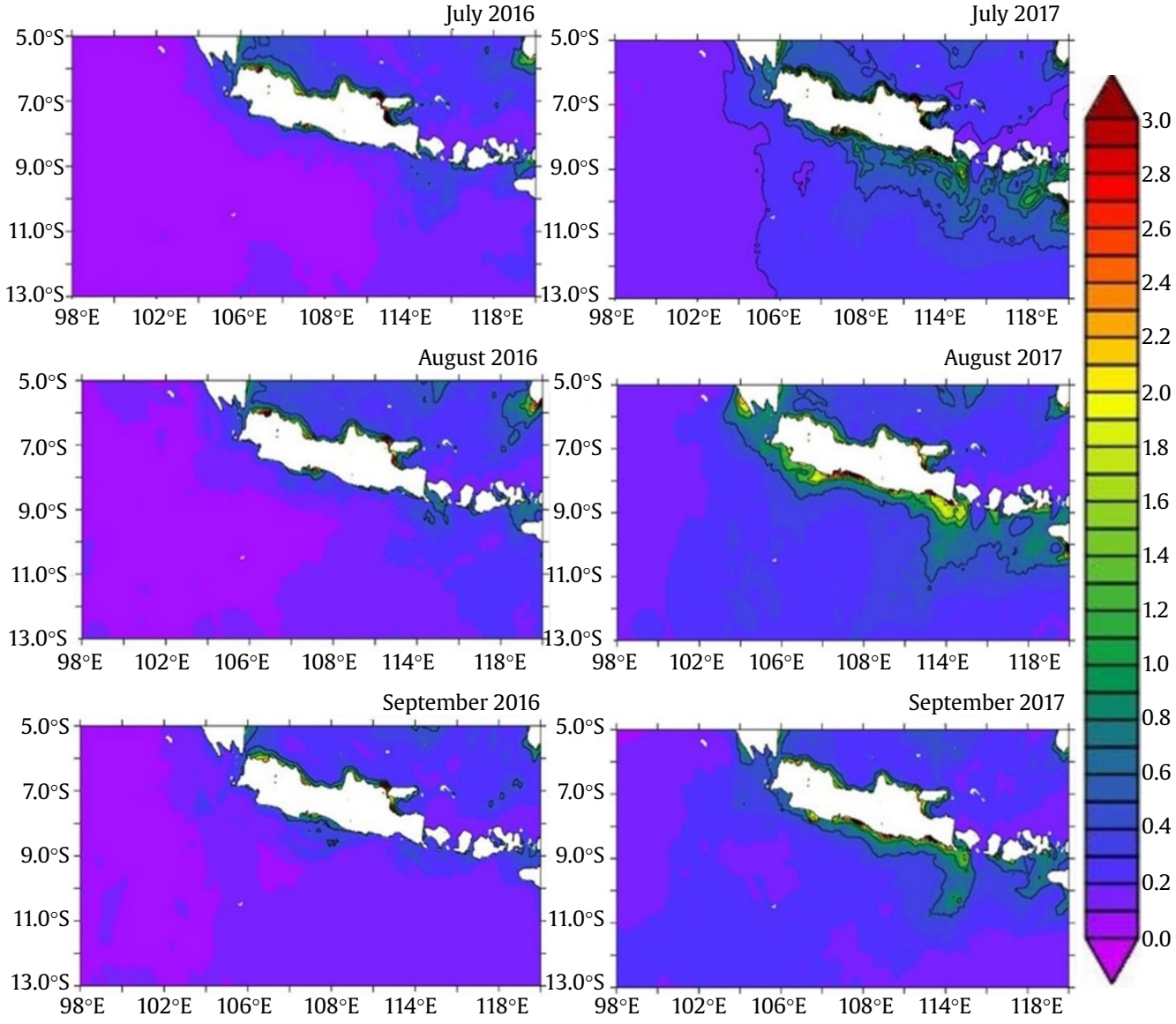

Figure 6. Monthly averaged of remotely-sensed Chl-a distribution (mg/m^3) during JAS 2016 and 2017

Java in September 2017. We noted that the HSI value decreases from 0.5 to 0.3 during the transition to the northwest monsoon from October to December 2017 (Figure 10). The lowest HSI prediction started to form in the south of West Java and the southern waters of Lampung in January 2017. Then the high HSI value of 0.5-0.6 recovered again in the south of Central Java and Bali Strait with smaller coverage in May 2017. Its value expands bigger coverage and formed in southern Central Java and southern Bali-Lombok Straits in June 2017 (Figure 10).

The extreme negative IOD in 2016 certainly affects the prediction pattern of fish distribution in the waters south of Java. The distribution of HSI value of 0.2-0.3 in JAS 2017 covers almost the entire study area in the southern waters of the Java-Lesser Sunda Islands, but in JAS 2016, it appears to have narrowed to a third. The HSI value of 0.5-0.6 itself covers only small areas, as

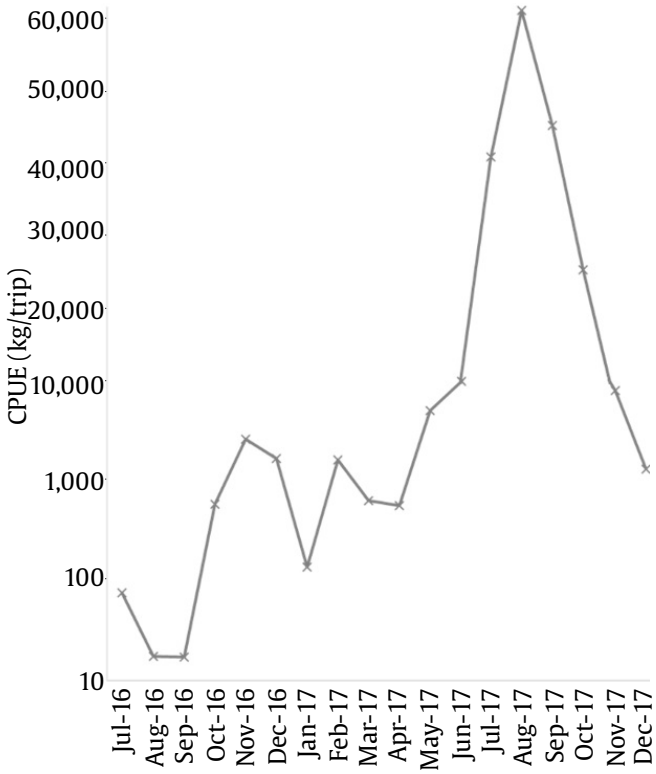

Figure 7. Variability of the calculated CPUE during July 2016-December 2017

appeared in the south of Central Java and Bali.

Validation of predicted HSI was carried out by plotting the geographic position of CPUE (black circle) and HSI in one map (Figure 9). However, the distribution of CPUE is still limited to fishing log-book data recorded at the Cilacap Fishing Port, which covers the most fishing activities in the southern waters of Central Java. The southern waters of East Java and Bali-Lombok Islands show a high HSI distribution (Figure 10), but no fishing log-book data are available for these areas. The distribution pattern of the predicted HSI corresponds moderately with CPUE data, indicating that GAM is good enough for modeling potential fishing grounds.

GAM plots (Figure 11) represent an individual effect of each predictor variable on CPUE. Rug plots on the horizontal axis represent observed data points, and the fitted function is shown by the full line. The dashed line shows the 95% confidence interval. The optimum positive effect on CPUE was observed from SST values of 26.9-27.2°C. Below 25.2°C and the range of 27.9-29.2°C result in negative effects on CPUE. SSS shows an optimum positive effect on CPUE at values of 33.7-34.0°/00. The optimum positive effect of SST and SSS represents the influence of Ekman pumping that brings cold and saltier waters from the deep layer to the surface layer. The positive effect of SSC started on 0.19 mg/m^3 where the optimum effect range between 0.19 until 0.21 mg/m^3. Beyond 0.21 mg/m^3, the positive effect of Chl-a on CPUE continued to increase with widening confidence intervals.

The decreasing trends are shown by EKE and MLD graphs that indicated a negative effect trend on CPUE. The EKE value characterizes the horizontal friction process caused by the complex topography and narrow straits, such as in the Bali-Lombok Straits. The positive effect of EKE on CPUE shows at a value below 200 cm^2/s^2. However, CPUE data in these waters were not available for HSI validation. MLD in the study area is influenced by the interaction between wind stress and the advection process, so the thin mixed layer indicates the effect of upwelling. Overall, SSC and SST have a significant role in determining suitable habitats for fishing activities in the upwelling area of southern Java where SSC is the most important habitat predictor for mackerel tuna migration in the southern coast of Java.

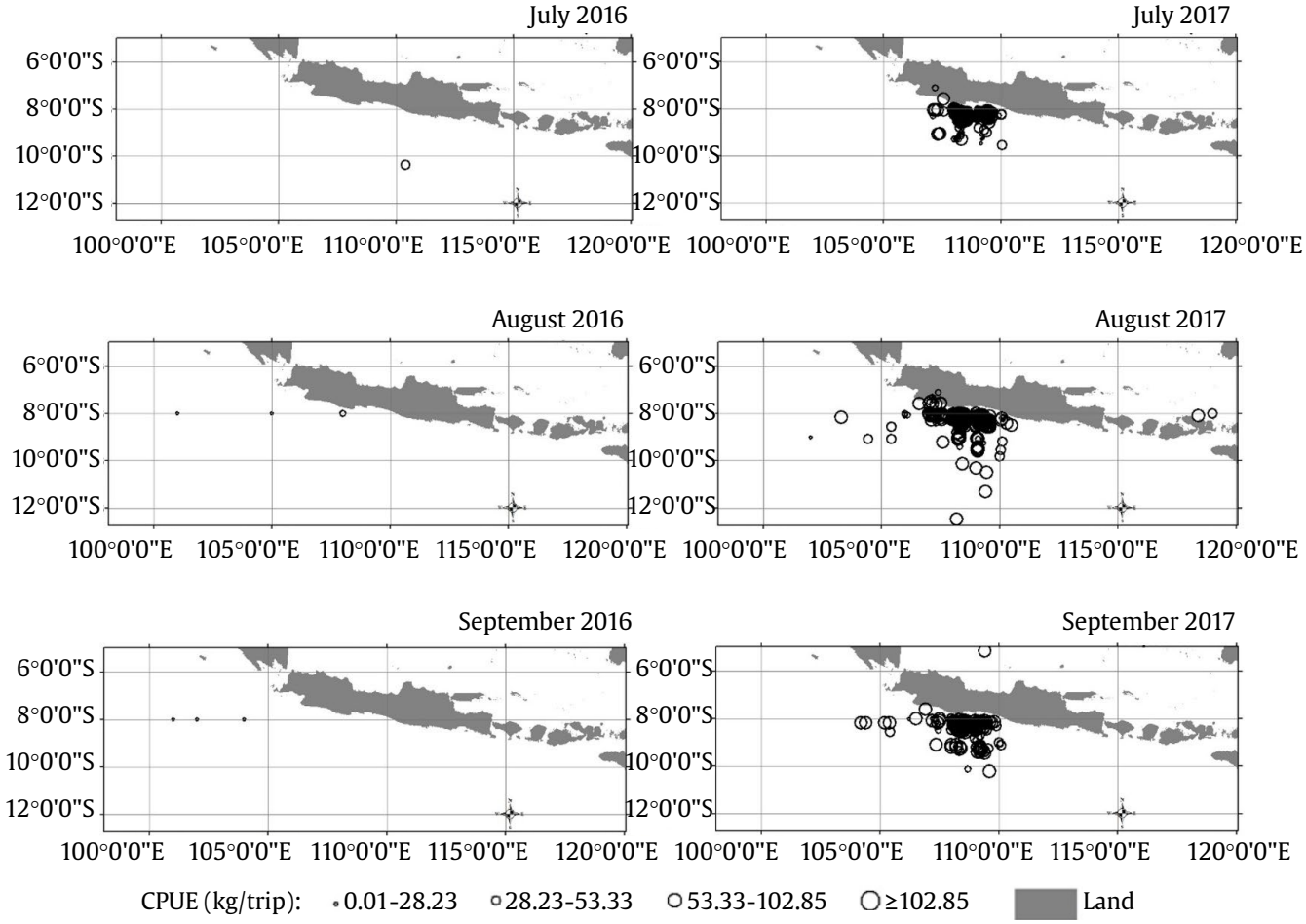

Figure 8. Monthly compilation of CPUE distribution during JAS 2016 and 2017

4. Discussion

The waters along the southern coast of Sumatra and Java are known as an upwelling region and productive fisheries grounds. The evolution of upwelling in the region could be detected by SST (satellite-derived ocean thermal) and remotely-sensed SSC. The present study shows that seasonal SSC is a consequence of monsoon-driven coastal upwelling, with higher and lower values of SSC occurring during upwelling and non-upwelling seasons. Several case studies also suggest that ENSO and IOD events have modulated the upwelling magnitude and SSC along the coast of Sumatra-Java Islands, as previously mentioned. It has been investigated that the negative IOD 2016 was the strongest negative IOD event (Lim and Hendon 2017; Lu *et al.* 2018) since 1980, according to NOAA Optimum Interpolation Sea Surface Temperature V2 dataset (OISSTv2; Reynolds *et al.* 2002), with the peak Indian Ocean Dipole Mode Index (DMI; Saji *et al.* 1999) reaching −1.5°C. Our analysis confirms the extreme negative IOD has forced the westerly wind

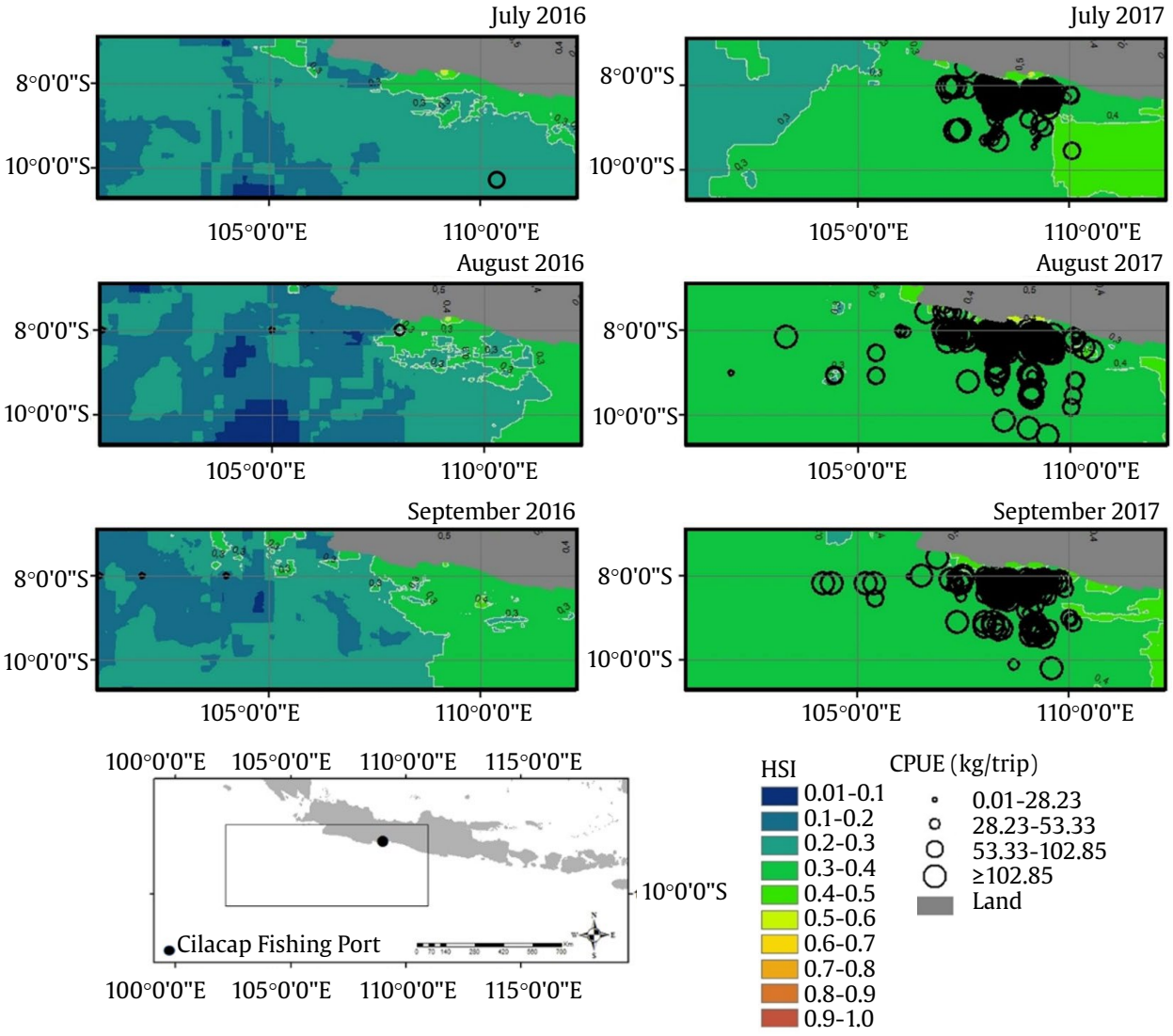

Figure 9. HSI prediction pattern of mackerel tuna overlaid with CPUE in the selected area of south Java during JAS 2016 and 2017

anomaly, the mixed layer thickening, even during the southeast monsoon period. This study found a weak southeasterly wind in JAS 2016 influenced by wind anomalies during extreme negative IOD. It is consistent with Lu *et al.* (2018) that the wind anomaly over the equatorial Indian Ocean reduced the magnitude of southeasterly wind off the Sumatran coast. Lim and Hendon (2017) also reported that the extreme negative IOD in 2016 resulted in a reversal of the monthly anomaly of 10 m zonal winds averaged over 5°S–5°N that located to the north of our study area. This study also supports several previous studies related to MLD impact on upwelling (Chen *et al.* 2006; Shulman *et al.* 2007; Du *et al.* 2008). Therefore, it produces the warmer SST and no Chl-a bloom, including low fish catch during extreme negative IOD in 2016..

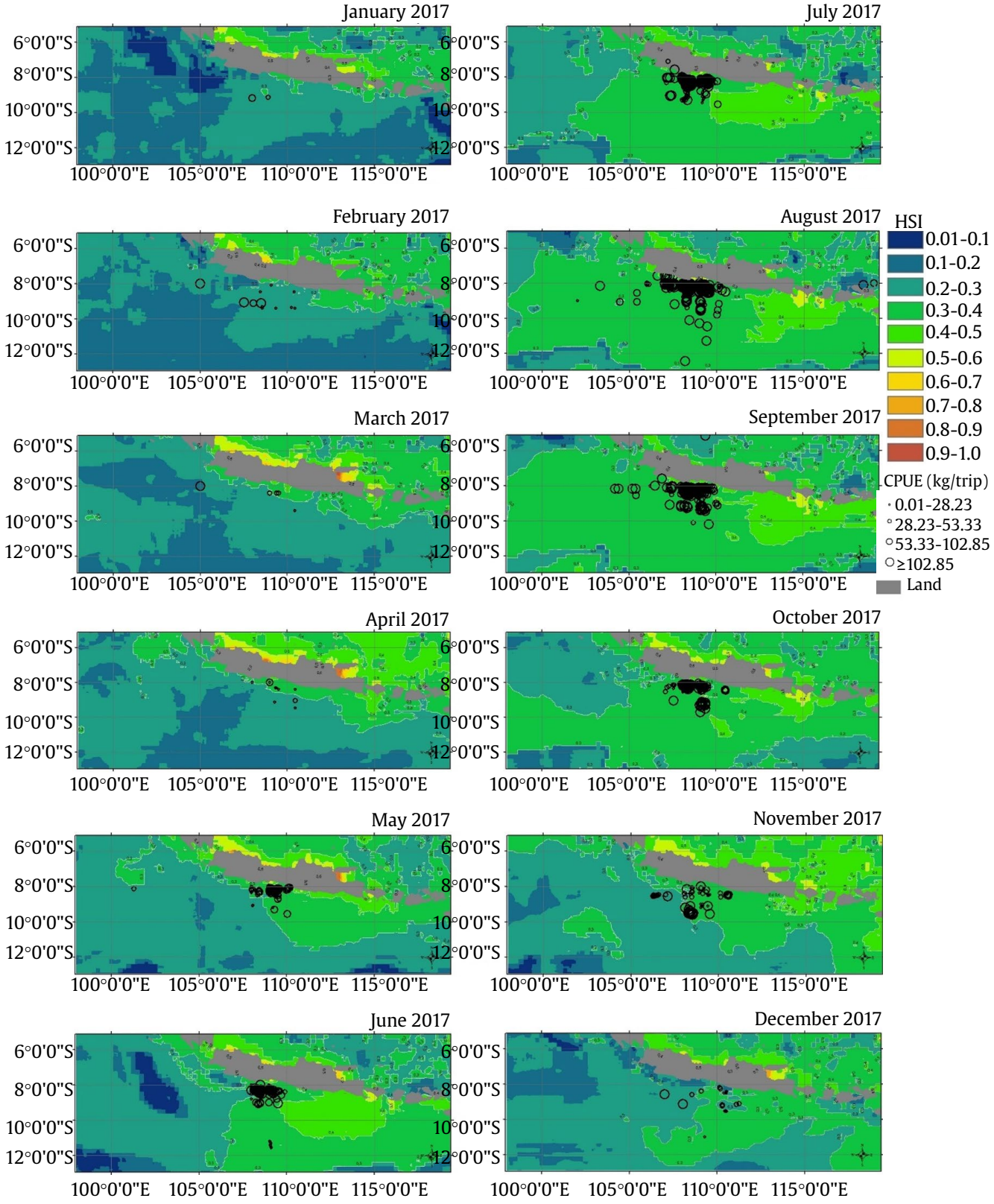

Figure 10. HSI prediction pattern of mackerel tuna overlaid with CPUE in the study area during 2017. Overestimating fishing predictions caused by overestimating remotely-sensed Chl-a concentrations in turbid waters are not included in the analysis, such as the Java Sea caused by many riverine inputs

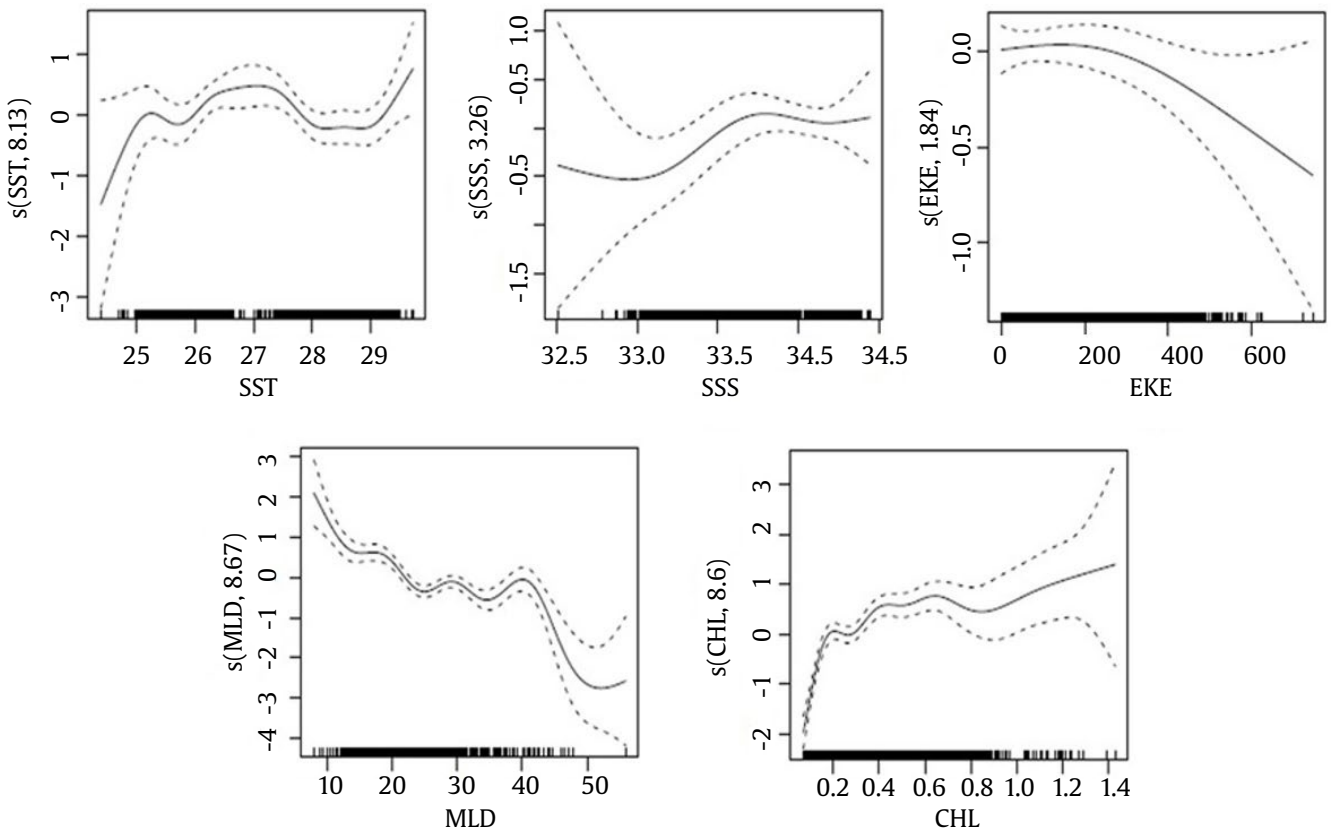

Figure 11. Effect of the five oceanographic parameters on CPUE, from the model constructed with SST, SSS, EKE, MLD, and SSC (CHL), as calculated by GAM. Rug plots on the horizontal axis represent predictors (oceanographic parameters), and the vertical axis represents a response scale (CPUE) with a smoothing estimator (s). The dashed line shows the 95% confidence interval

Based on the Oceanic Niño Index (ONI), the year 2017 was influenced by a weak La Nina, starting from October 2017 to December 2017, with an anomaly of -0.7° to -1.0°C [Huang *et al.* 2017, ONI data can be accessed on Climate Prediction Center-ONI (noaa.gov)]. In normal years, Susanto *et al.* (2001) reported that upwelling occurs from early June to mid-October which started from southern East Java and shifted towards the northwest. In line with this information, our findings show a high value of CPUE from May to November 2017, despite the CPUE itself not being free from sampling bias which depended on the fishermen's choice of fishing locations.

Fish occurrence and abundance often adopt from the CPUE Data as an index (Lehodey *et al.* 1998), so the high CPUE could indicate preferred oceanographic conditions for a species. This study examines model results of HSI and their relevance as environmental indicators of mackerel tuna habitat. A high value of HSI distribution (shaded yellow in Figure 10) is shown along the coast of southern Central Java between May until August 2017 and is consistent with the CPUE data. The extreme negative IOD impact, in this case, produces a small coverage area of the high value in the region during the southeast monsoon in JAS 2016. On the other hand, Lumban-Gaol *et al.* (2021) reported that positive IOD increased upwelling intensity while negative IOD increased downwelling intensity in the region. They noted that the difference in total small pelagic fish catch between positive IOD and negative IOD could reach five times.

Our findings suggest a strong mixing at the entrance of Lombok Strait has significantly increased the HSI in the region. This mixing is mainly driven by internal tide-induced turbulence, as reported by previous studies using in situ observations (Koch-Larrouy *et al.* 2015; Bouruet-Aubertot *et al.* 2018; Purwandana *et al.* 2020; Purwandana *et al.* 2021). The availability of fishing log-book in this region will improve the calculating processes in GAM. Related to the CPUE, it is also interesting to examine the impact of extreme negative IOD in reducing the mixing. At last, the seasonal coastal upwelling and the effect of

IOD modulations are essential features for mackerel tuna habitat.

Understanding climate variability is fundamental for fisheries management in the study area. In this case, GAM results can be a tool in simplifying complex environmental dynamics processes and strengthening operational services for efficiency in fishing efforts. We found that the most significant habitat predictor for mackerel tuna migration in the southern coast of Java is SSC, followed by SST with an optimum range of 0.19-0.21 mg/m^3 and 26.9-27.2°C, respectively. Therefore, the present study provides a simple way for determining future potential fishing ground for mackerel tuna migration in the southern coast of Java by using satellite data or model prediction for SSC and SST parameters. Our finding is similar to a recent paper on skipjack tuna in the Gulf of Bone-Flores Sea (Zainuddin *et al.* 2017) that reported the optimum positive effect of remotely-sensed SSC of 0.2 mg/m^3 on CPUE. Concerning future prediction, the climate variability tends to consider ENSO has a less significant impact on the seasonal Ekman dynamics than IOD in the southern coast of Java (Wirasatriya *et al.* 2020), where the IOD events often lag ENSO by 6-11 months (Xu *et al.* 2021). Nowadays, the model accuracy for IOD prediction is becoming robust by further improving several forecasting models, as reported by Lu *et al.* (2018) and Lim and Hendon (2017). In the future, the present model result of HSI still needs additional CPUE data from other fishing ports along the west coast of Sumatra and south of Java-Lesser Sunda Islands. Integration of much CPUE data supports gaining accuracy of the optimum positive effect on CPUE from the key parameters such as Chl-a and SST. Then the validation can be done through collaboration with fisherfolk, especially during their fishing activities.

Acknowledgements

This study is partially supported by Big Data and Ocean Modeling (BiOM) Laboratory, Department of Marine Science and Technology, IPB University. We wish to acknowledge the use of ArcGIS software at the Division of Marine Remote Sensing and Geographic Information System, Department of Marine Science and Technology, Faculty of Fisheries and Marine Sciences, IPB University.

References

Báez JC *et al.* 2020. Climatic oscillations effect on the yellowfin tuna (*Thunnus albacares*) Spanish captures in the Indian Ocean. *Fisheries Oceanography* 29: 572-583. DOI:10.1111/fog.12496

Bouruet-Aubertot P *et al.* 2018. Contrasted turbulence intensities in the Indonesian throughflow: a challenge for parameterizing energy dissipation rate. *Ocean Dynam* 68:1–75. DOI:10.1007/s10236-018-1159-3

Chen CC *et al.* 2006. Winter phytoplankton blooms in the shallow mixed layer of the South China Sea enhanced by upwelling. *JMS* 59:97–110.

Chen IC *et al.* 2005. Distribution of albacore (*Thunnus alalunga*) in the Indian Ocean and its relation to environmental factors. *J Fish Oceano* 14:71–80.

Chen G *et al.* 2016. Interannual variability of equatorial eastern Indian Ocean upwelling: local versus remote forcing. *J Phys Oceanogr* 46:789–807.

Du Y *et al.* 2008. Interannual variability of sea surface temperature off Java and Sumatra in a Global GCM. *JCL* 21:2451-2465. DOI:10.1175/2007JCLI1753.1

Gordon AL, Susanto RD. 2001. Banda sea surface-layer divergence. *Ocean Dynamics* 52:2-10.

Howell EA, Kobayashi DR. 2006. El Nin˜o effects in the palmyra atoll region: oceanographic changes and bigeye tuna (*Thunnus obesus*) catch rate variability. *J Fish Oceano* 15:477–489.

Huang B *et al.* 2017. Extended reconstructed sea surface temperature, version 5 (ERSSTv5): upgrades, validations and intercomparisons. *J Clim* 30:8179-8205.

Iskandar I *et al.* 2018. Evolution and impact of the 2016 negative Indian Ocean Dipole. *J Phys: Conf Ser* 985: 01201.

Kämpf J, Kavi A. 2019. SST variability in the eastern Intertropical Indian Ocean-on the search for trigger mechanisms of IOD events. *Deep Sea Research Part II: Topical Studies in Oceanography* 166:67-74. DOI:10.1016/j.dsr2.2018.11.010

Koch-Larrouy A *et al.* 2015. Estimates of tidal mixing in the Indonesian archipelago from multidisciplinary INDOMIX *in-situ* data. *Deep Res Part I Oceanogr Res Pap* 106:136–153. DOI:10.1016/j.dsr.2015.09.007

Lahlali H *et al.* 2018. Environmental aspects of tuna catches in the Indian Ocean, southern coast of Java, based on satellite measurements. *In: 2018 4th International Symposium on Geoinformatics (ISyG)*. Malang: IEEE. pp. 1-6. DOI:10.1109/ISYG.2018.8612020

Lan KW, *et al.* 2013. Effects of climate variability on the distribution and fishing conditions of yellowfin tuna (*Thunnus albacares*) in the western Indian Ocean. *Climatic Change* 119:63-77. DOI:10.1007/s10584-012-0637-8

Lehodey P *et al.* 1998. Predicting skipjack tuna forage distributions in the equatorial Pacific using a coupled dynamical bio-geochemical model. *Fish Oceanogr* 7:317–325.

Lim EP, Hendon HH. 2017. Causes and predictability of the negative Indian Ocean Dipole and its impact on lanina during 2016. *Nature* 7:1-11. DOI:10.1038/s41598-017-12674-z

Lu B *et al.* 2018. An extreme negative Indian Ocean Dipole event in 2016: dynamics and predictability. *Climate Dyn* 51:89-100. DOI:10.1007/s00382-017-3908-2

Lumban-Gaol J *et al.* 2015. Variability of satellite-derived sea surface height anomaly, and its relationship with bigeye tuna (*Thunnus obesus*) catch in the Eastern Indian Ocean. *European Journal of Remote Sensing* 48:465-477. DOI:10.5721/EuJRS20154826

Lumban-Gaol J *et al.* 2021. Impact of the strong downwelling (upwelling) on small pelagic fish production during the 2016 (2019) negative (positive) Indian Ocean Dipole Events in the Eastern Indian Ocean off Java. *Climate* 9:1-11. DOI:10.3390/cli9020029

Mugo R *et al.* 2010. Habitat characteristics of skipjack tuna (*Katsuwonus pelamis*) in the Western North Pacific: a remote sensing perspective. *J Fish Oceano* 19: 382-396.

Nur'utami MN, Hidayat R. 2016. Influences of IOD and ENSO to Indonesian rainfall variability: role of atmosphere-ocean interaction in the Indo-pacific Sector. *Procedia Environmental Sciences* 33:196-203. DOI:10.1016/j.proenv.2016.03.070

Potemra JT *et al.* 2003. Observed estimates of convergance in the Savu Sea, Indonesia. *Journal of Geophysical Ressearch* 108: 1-11.

Purwandana A *et al.* 2020. Spatial structure of turbulent mixing inferred from historical CTD datasets in the Indonesian seas. *Prog Oceanogr* 184:102312. DOI:10.1016/j.pocean.2020.102312

Purwandana AY *et al.* 2021. Observation of internal tides, nonlinear internal waves and mixing in the Lombok Strait, Indonesia. *Continental Shelf Research* 216:104358.

R Core Team. 2018. R: a language and environment for statistical computing. R Foundation for Statistical Computing, Vienna, Austria. Available at: http://www.R-project.org/ [Date accessed: 1 October 2018]

Rachman HA *et al.* 2020. Influence of coastal upwelling on sea surface temperature trends Banda Sea. *IOP Conf Ser: Earth Environ Sci* 429:012015.

Reynolds RW *et al.* 2002. An improved in situ and satellite SST analysis for climate. *J Clim* 15:1609–1625.

Saji NH *et al.* 1999. A dipole mode in the Tropical Indian Ocean. *Nature* 401:360–363.DOI:10.1038/43854

Schlitzer R. 2021. Ocean Data View. Available at: https://odv.awi.de [Date accessed: 1 June 2017]

Shulman I *et al.* 2007. Modeling of upwelling/relaxation events with the Navy Coastal Ocean Model. *J Geophys Res* 112:1-12. DOI:10.1029/2006JC003946

Sparre P, Venema SC. 1999. *Introduction to Tropical Fish Stock Assesment*. Rome: FAO Fisheries Department.

Susanto RD *et al.* 2001. Upwelling along the coasts of Java and Sumatra and its relation to ENSO. *Geophysical Research Letters* 28:1599–1602.

Syamsuddin M *et al.* 2016. Interannual variation of bigeye tuna (*Thunnus obesus*) hotspots in the eastern Indian Ocean off Java. *Int J Remote Sens* 37:2087–2100.

Taufikurahman Q, Hidayat R. 2017. Coastal upwelling in Southern Coast of Sumbawa Island, Indonesia. *IOP Conf Ser: Earth Environ Sci* 54:012075.

Varela R *et al.* 2016. Influence of coastal upwelling on SST trends along the South Coast of Java. *PLOS ONE* 11:e0162122.

Wang M *et al.* 2017. Mechanism of seasonal eddy kinetic energy variability in the Eastern Equatorial Pacific Ocean. *J Geophys Res* 122:3240-3252. DOI:10.1002/2017JC012711

Wirasatriya A *et al.* 2020. Ekman dynamics variability along the southern coast of Java revealed by satellite data. *Int J Remote Sens* 41:8475–8496.

Wiryawan B *et al.* 2020. Catch per unit effort dynamic of yellowfin tuna related to sea surface temperature and chlorophyll in Southern Indonesia. *Fishes* 5:28 DOI:10.3390/fishes5030028

Wood SM. 2006. *Generalized Additive Models, An Introduction with R*. London: Chapman and Hall.

Wu YL *et al.* 2020. Determining the effect of multiscale climate indices on the global yellowfin tuna (*Thunnus albacares*) population using a time series analysis. *Deep Sea Research Part II: Topical Studies in Oceanography* 175:104808. DOI:10.1016/j.dsr2.2020.104808

Wyrtki K. 1961. *Physical Oceanography of the Southeast Asian Waters*. San Diego: University of California.

Xu T *et al.* 2021. Satellite-observed multi-scale variability of sea surface chlorophyll-a concentration along the South Coast of the Sumatra-Java Islands. *Remote Sens* 13:2817.

Zainuddin M *et al.* 2008. Albacore (*Thunnus alalunga*) fishing ground in relation to oceanographic conditions in the western North Pacific Ocean using remotely sensed satellite data. *Fish Oceanogr* 17:61–63.

Zainuddin M *et al.* 2017. Detection of pelagic habitat hotspots for skipjack tuna in the Gulf of Bone-Flores Sea, southwestern Coral Triangle tuna, Indonesia. *PLoS ONE* 12:e0185601. DOI:10.1371/journal. pone.0185601

Zagaglia CR *et al.* 2004. Remote sensing data and longline catches of yellowfin tuna (*Thunnus alalunga*) in the Equatorial Atlantic. *Remo Sen Enviro* 93:267–281.